Linear instability or buckling problems for mechanical and coupled thermomechanical extreme conditions

Adnan Ibrahimbegovic[*1], Emina Hajdo[1,2] and Samir Dolarevic[2]

[1] *Laboratoire de mécanique et technologie, École Normale Supérieure,*
61 Avenue du Président Wilson, 94230 Cachan, France
[2] *Faculty of Civil Engineering, University of Sarajevo, Patriotske lige 30,*
71000 Sarajevo, Bosnia and Herzegovina

Abstract. In this work we propose a novel procedure for direct computation of buckling loads for extreme mechanical or thermomechanical conditions. The procedure efficiency is built upon the von Karmann strain measure providing the special format of the tangent stiffness matrix, leading to a general linear eigenvalue problem for critical load multiplier estimates. The proposal is illustrated on a number of validation examples, along with more complex examples of interest for practical applications. The comparison is also made against a more complex computational procedure based upon the finite strain elasticity, as well as against a more refined model using the frame elements. All these results confirm a very satisfying performance of the proposed methodology.

Keywords: buckling; thermomechanical coupling; geometric instability, critical load, eigenvalue problem

1. Introduction

One of the most frequent cases of extreme loading conditions that engineering structures can be exposed to, pertains to fire. The most sadly famous example, the World Trade Center collapse in September 2001, is certainly not the only one. One can cite a number of catastrophic failures under combined action of mechanical and thermal loads, such as MGM Grand Hotel in 1980 in Nevada, First Interstate Bank in Los Angeles in 1988 or Windsor Tower in Madrid in 2005.

Each of these failures has been caused by the same mechanism of combined action of mechanical loading and high temperature. Hence, for the predictive analysis of the phenomena of this kind we ought to provide the correct representations of two different failure mechanisms. The first one pertains to softening material failure under temperature increase (e.g., Van Ngo *et al.* (2013)), and the second one pertains to geometric instability phenomena brought about the critical values of mechanical and thermal load. The latter failure mechanism pertaining to buckling and its correct representation are studied in detail in this work.

In particular, we seek to provide as simple as possible and yet sufficiently predictive model for

---

*Corresponding author, Professor, E-mail: adnan.ibrahimbegovic@ens-cachan.fr

instability failure under extreme mechanical or thermomechanical loads. We take for simplicity the mechanical systems built of truss or frame in order to illustrate the details of the proposed coupled system instability computational procedure. However, the proposed method would directly apply to more complex mechanical systems.

The main novelty concerns the proposed model for thermomechanical coupling based upon the von Karman strain measure to account for geometric nonlinearities, along with the corresponding generalized eigenvalue problem for direct estimate of the critical load leading to instability and failure. Each of model ingredients has been until now studied separately, but never before combined within a single predictive model as proposed herein. Namely, the previous studies of thermomechanical coupling have been carried out either in small strain framework that precludes the geometric instabilities and only account for temperature dependence of material parameters (e.g., see Ibrahimbegovic and Chorfi (2002) for steel, Ibrahimbegovic *et al*. (2005) for cellular masonry materials or Ngo *et al*. (2013) for damage of concrete). Similarly, geometric instabilities are studied only for slender elastic structures, for either small (e.g., Ibrahimbegovic *et al*. (1996)), or large pre–buckling displacements (Ibrahimbegovic and Al Mikdad (2000), Dujc *et al*. (2010)) with no specific development as presented herein. The latter departs from these general studies of instability phenomena in seeking efficiency by using the von Karman strain measure that is intrinsically connected to buckling problems and results with general eigenvalue problem where solution directly leads to critical buckling load. The resulting computational efficiency is the main advantage with respect to the most general approach combining the large displacements and temperature effect (e.g., Yang *et al*. (2008)), which require very complex and costly computational procedure (Ibrahimbegovic and Al Mikdad (2000), Ibrahimbegovic *et al*. (1996, 2001)). Moreover, provided that the main hypothesis on small pre-buckling displacement is valid, the procedure proposed here will apply to any kind of material response.

The outline of the paper is as follows. In the next section we briefly recall the basics of heat transfer problem. We discuss both nonstationary case, which can lead to the mechanical properties reduction, as well as the stationary case which can produce internal forces in the structural elements. In Section 3, we present the proposed geometrically nonlinear framework based upon the von Karman strain measure, resulting with the general linear eigenvalue problem. Section 4 provides a brief summary of the final problem formulation in terms of general linear eigenvalue problem, different methods for its efficient solution procedure and in particular the power method and subspace iteration method. The results of several illustrative numerical examples are presented and discussed in Section 5. The concluding remarks are stated in Section 6.

2. Thermoelasticity

The phenomena of thermomechanical coupling are very important in terms of accounting properly for temperature induced change of material parameters. We are also interested in computation of thermally induced deformations, as well as in detecting a critical thermal loading that causes buckling phenomena.

For simplicity, we start with the constitutive model of thermoelasticity, which must be able to account for both mechanics and thermal effects. We consider a simple 1D problem of thermomechanical coupling, defined in the domain $x \in [0, l]$. We briefly review the classical model of small strain thermoelasticity. First, the two equations derived in purely mechanics case that also apply to the present coupled thermomechanics framework, pertaining to equilibrium and

kinematics

$$\frac{\partial \sigma}{\partial x} + b = 0 \qquad \varepsilon = \frac{\partial u}{\partial x} \tag{1}$$

where σ is stress, b distributed load, ε is strain and u is displacement. One dimensional heat equation for the stationary case is given as

$$-\frac{\partial q}{\partial x} + r = 0 \qquad q = -k\frac{\partial \theta}{\partial x} \tag{2}$$

where r is the external heat supply, q is outgoing heat flux, k is the diffusion coefficient and θ is temperature.

The nonstationary case is based on the first principle of thermodynamics (e.g., Ericksen (1998), Ibrahimbegovic (2009)), which states that any change of the internal energy is proportional to the combined effects of the stress power and the heat supply

$$\frac{\partial}{\partial t} e(\varepsilon, s) = \sigma \frac{\partial \varepsilon}{\partial t} + r - \frac{\partial q}{\partial x} \tag{3}$$

where e is specific internal energy, and s is its state-variable of entropy.

We can avoid working with entropy as the state variable, by exploiting the Legendre transformation in order to introduce the free energy of Helmholtz $\psi(\varepsilon, \theta)$

$$\psi(\varepsilon, \theta) = e(\varepsilon, s) - s\theta \quad , \quad \theta = \frac{\partial e}{\partial s} \tag{4}$$

The first principle of the thermodynamics can then be described as follows

$$\underbrace{\left(\frac{\partial \psi}{\partial \varepsilon} - \sigma\right)}_{=0}\frac{\partial \varepsilon}{\partial t} + \underbrace{\left(\frac{\partial \psi}{\partial \theta} + s\right)}_{=0}\frac{\partial \theta}{\partial t} + \theta\frac{\partial s}{\partial t} = r - \frac{\partial q}{\partial x} \tag{5}$$

Varying independently the state variables, ε and θ, we obtain the constitutive equation for stress and entropy, along with a reduced form of the first principle

$$\sigma = \frac{\partial \psi}{\partial \varepsilon}; \quad s = -\frac{\partial \psi}{\partial \theta}; \quad \theta\frac{\partial s}{\partial t} = r - \frac{\partial q}{\partial x} \tag{6}$$

Local balance and energy equations are then reduced to

$$0 = \frac{\partial \sigma}{\partial x} + b \qquad 0 = \theta\frac{\partial s}{\partial t} + \frac{\partial q}{\partial x} - r \tag{7}$$

In the numerical implementation it is more convenient to use the weak form of these equations

$$0 = G_M(\varepsilon, \theta; w) := \int_l \left(\frac{dw}{dx}\sigma + wb\right)dx + w(l)\overline{t} \tag{8}$$

$$0 = G_T(\varepsilon, \theta; \omega) := \int_l \left[\omega\left(\theta\frac{\partial s}{\partial t} - r\right) - \frac{d\omega}{dx}q\right]dx - \omega(l)\overline{q} \tag{9}$$

where *w* and *ω* are virtual displacement and virtual temperature field, respectively. The weak form written above holds for a bar of length *l*, with the left end clamped and maintained at a fixed temperature, and the right end loaded by traction $\bar{t}$ and submitted to imposed heat flux $\bar{h}$.

If we consider the fire of long duration (e.g., World Trade Center), we can count with diffusion phenomena to remove the temperature field time-dependence ($\partial\theta/\partial t = 0$) and thus obtain the stationary heat transfer problem.

For an elastic truss bar and the corresponding thermomechanical problem, stress equation is given by

$$\sigma = E\left(\varepsilon - \varepsilon_{th}\right) = \sigma_m + \sigma_{th} \quad ; \quad \varepsilon_{th} = \alpha\theta \tag{10}$$

We note in passing that these results can further be generalized to elastoplastic case (e.g., Ngo *et al.* (2013)), where we can further allow for the appearance of plastic strain which can reduce the stress–producing strain to its elastic component only, $\varepsilon^e = \varepsilon - \varepsilon^p$. The plastic strain evolution is described by yield criterion with plastic regime also contributing the plastic dissipation $D = \sigma\dot{\varepsilon}^p$ as the additional heat source. All the material parameter defining the elastic and plastic regime can be temperature dependent, such as $E(\theta)$ or $\sigma_y(\theta)$ which can further affect the critical loading.

3. Geometric instability problem

The geometric instability problem pertains to the structures that can undergo critical equilibrium state taking it from stable to unstable. The latter implies that a small change in loads can lead to a disproportional change in structural response, and it is usually associated with the singularity of the structure stiffness matrix. Geometric instability in general implies that there is a risk of large (or moderate) structural motion such that kinematics and equilibrium equations ought to be taken as nonlinear. The structure stiffness matrix in this case will have two parts: usual term often referred to as material part and external loading proportional term referred to as geometric stiffness. The last part can thus cause the structural stiffness singularity for the case of the structure with compressed structural elements.

The most efficient approach for dealing with geometric instability phenomena can be provided for buckling, considering small pre–buckling displacements before reaching the critical equilibrium state. In that case, we can still consider linear kinematics and only turn to nonlinear equilibrium equations. More precisely this implies that equilibrium equations are set in the deformed configuration if we compute the solution by using the strong (local) form of these equations. A number of classical results for buckling loads were computed in this manner for simple structures, and reported in standard reference books (e.g., Timoshenko and Gere (1962)).

However, when computing the solution by using the finite element method, we typically take weak (integral) form of the problem. This allows us to tackle a much more complex problem, but at price to obtain only an approximate solution. The quality of such an approximate solution can always be improved by refining the mesh in the standard manner of the finite element method. We show here that such an approach can be developed in a very systematic manner for dealing with buckling problems of large diversity of complex structures by using the von Karman deformation measure.

The von Karman deformation measure is well suited for typical structural mechanics problems in geometrically nonlinear response where the deformations are small and rotations are moderate. For clarity, we choose here the simplest such model of truss-bar. In such a case, the infinitesimal

strain measure, $\varepsilon = du_1 / dx$ (where u_1 is the bar axial displacement), remains much smaller than infinitesimal rotation $\omega = du_2 / dx$ (where u_2 is the transverse displacement).

Thus, we ought to use a geometrically nonlinear measure of deformation, with additional term as square of the rotation, which is the same order of magnitude as the infinitesimal dilatation. Such deformation measure, first proposed by von Karman (e.g., see Bathe (1996)), can be written as

$$E^{vk} = \frac{du_1}{dx} + \frac{1}{2}\left(\frac{du_2}{dx}\right)^2 \tag{11}$$

where u_1 is displacement along the bar and u_2 is transverse displacement. We can easily show that such an expression is the second order approximation to the stretch, which is the true nonlinear measure of large strain (e.g., see Ibrahimbegovic (2009)) we refer to Fig. 1 for ilustration.

$$ds_v = \sqrt{dx^2 + dv^2} = dx\sqrt{1+\left(\frac{dv}{dx}\right)^2} \approx dx\left(1+\frac{1}{2}\left(\frac{dv}{dx}\right)^2\right) \rightarrow E^{vk}_{(v)} = \frac{ds_v - dx}{dx} = \frac{1}{2}\left(\frac{dv}{dx}\right)^2 \tag{11a}$$

$$ds_u = dx + du \qquad \rightarrow \qquad E^{vk}_{(u)} = \frac{ds_u - dx}{dx} = \frac{du}{dx}$$

With the real von Karman deformation defined as quadratic form in transverse displacement, the virtual strain measure of the same kind will remain a function of that displacement. We can compute the virtual von Karman deformation by using the Gâteaux or directional derivative formulation (e.g., see Ibrahimbegovic (2009)). In particular, we introduce the displacements in the perturbed configuration

$$u_{1\alpha} = u_1 + \alpha w_1$$
$$u_{2\alpha} = u_2 + \alpha w_2 \tag{12}$$

where w_1 and w_2 are corresponding virtual displacements in direction x_1 and x_2. The Gâteaux derivative computation in the direction of these virtual displacements leads to

$$\varepsilon^{vk} = \frac{d}{d\alpha}\left[E^{vk}\left(u_{1\alpha}, u_{2\alpha}\right)\right]\bigg|_{\alpha=0} = \frac{d}{d\alpha}\left[\frac{du_{1\alpha}}{dx} + \frac{1}{2}\left(\frac{du_{2\alpha}}{dx}\right)^2\right]\bigg|_{\alpha=0} \tag{13}$$

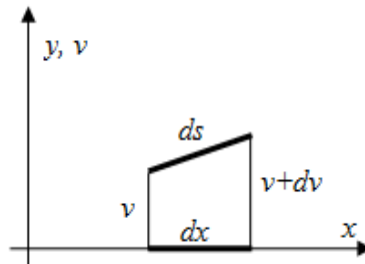$$= \frac{dw_1}{dx} + \frac{du_2}{dx}\frac{dw_2}{dx}$$

Fig. 1 The graphic illustration of von Karman strain measure

The weak form of such an instability problem can thus be defined by the following set of equations

kinematic equation: $\qquad \varepsilon(x) = \dfrac{du_1}{dx}$

constitutive equation: $\qquad \sigma(x) = E\left(\varepsilon(x) - \varepsilon_{tr}\right) \qquad \rightarrow \qquad N = A\sigma$

$$\text{(14)}$$

equilibrium equation: $\qquad \displaystyle\int_0^l \varepsilon^{vk} N dx = f^{ext}$

By combining the last three equations into a single one, we can also write an explicit form of the variational equation

$$\int_0^l \frac{dw_1}{dx} EA \frac{du_1}{dx} dx + \int_0^l \frac{du_2}{dx} \frac{dw_2}{dx} \underbrace{EA\left(\frac{du_1}{dx} - \alpha\theta\right)}_{N} dx = f^{ext} \tag{15}$$

We will use a two-node truss-bar finite element (see Fig. 2) for constructing the finite element approximations. Thus we can write the real displacement field interpolation

$$u_1(x) = N_1(x)u_{11} + N_2(x)u_{21}$$
$$u_2(x) = N_1(x)u_{12} + N_2(x)u_{22} \tag{16}$$

Where $N_1(x)$ and $N_2(x)$ are linear shape functions (see Fig. 2). In the spirit of Galerkin's method, the same kind of interpolation is chosen for the virtual displacement field

$$w_1(x) = N_1(x)w_{11} + N_2(x)w_{21}$$
$$w_2(x) = N_1(x)w_{12} + N_2(x)w_{22} \tag{17}$$

Given this simple choice of interpolation with shape functions as linear polynomials, we can easily obtain the corresponding derivatives

$$\frac{dN_1(x)}{dx} = -\frac{1}{l} \qquad \frac{dN_2(x)}{dx} = \frac{1}{l} \tag{18}$$

We can thus obtain the discrete approximations of the displacement derivatives that will be constant in each element
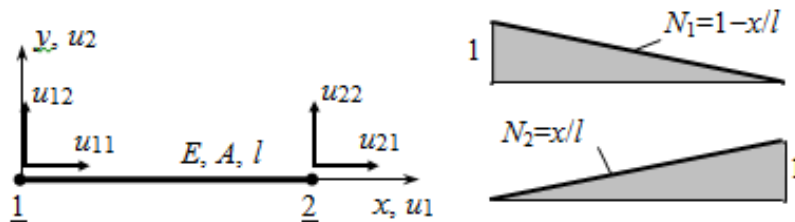

Fig. 2 Truss-bar 2-node element and shape functions

$$\frac{du_1}{dx}(x) = \sum_{a=1}^{n} \frac{dN_a(x)}{dx} u_{a1} = \frac{u_{21} - u_{11}}{l}$$

$$\frac{du_2}{dx}(x) = \sum_{a=1}^{n} \frac{dN_a(x)}{dx} u_{a2} = \frac{u_{22} - u_{12}}{l}$$

$$(19)$$

We gather nodal values of real displacements and virtual displacements, inside the corresponding vectors

$$\{d^e\} = \{u_{11} \quad u_{12} \quad u_{21} \quad u_{22}\}^T$$

$$\{w^e\} = \{w_{11} \quad w_{12} \quad w_{21} \quad w_{22}\}^T$$

$$(20)$$

The corresponding displacements derivatives can be further arranged in a strain–displacement matrix $\mathbf{B}$, which can be written as

$$\frac{du_1}{dx}(x) = \mathbf{B}_1^e \mathbf{d}^e \qquad \frac{dw_1}{dx}(x) = \mathbf{w}^{eT} \mathbf{B}_1^{eT}$$

$$\mathbf{B}_1^e = \left\{ \frac{dN_1}{dx} \quad 0 \quad \frac{dN_2}{dx} \quad 0 \right\} = \frac{1}{l} \{-1 \quad 0 \quad 1 \quad 0\}$$

$$\frac{du_2}{dx}(x) = \mathbf{B}_2^e \mathbf{d}^e \qquad \frac{dw_2}{dx}(x) = \mathbf{w}^{eT} \mathbf{B}_2^{eT}$$

$$\mathbf{B}_2^e = \left\{ 0 \quad \frac{dN_1}{dx} \quad 0 \quad \frac{dN_2}{dx} \right\} = \frac{1}{l} \{0 \quad -1 \quad 0 \quad 1\}$$

$$(21)$$

With this result on hand we can obtain the material part of the structure stiffness matrix leading to

$$I_1 = \int_0^l \left(\frac{dw_1}{dx} \right)^T EA \frac{du_1}{dx} dx = \int_0^l \mathbf{w}^T \mathbf{B}_1^T EA \mathbf{B}_1 \mathbf{d} dx = \mathbf{w}^T \underbrace{\int_0^l \mathbf{B}_1^T EA \mathbf{B}_1 dx}_{\mathbf{K}_m^e} \mathbf{d}$$

$$(22)$$

For the chosen approximation with 2-node truss-bar element, the material stiffness matrix can be written explicitly as

$$\mathbf{K}_m^e = \frac{EA}{l} \begin{bmatrix} 1 & 0 & -1 & 0 \\ 0 & 0 & 0 & 0 \\ -1 & 0 & 1 & 0 \\ 0 & 0 & 0 & 0 \end{bmatrix}$$

$$(23)$$

The geometric part of the structure stiffness matrix can then be written as follows

$$I_2 = \int_0^l \frac{dw_2}{dx} \frac{du_2}{dx} N dx = \int_0^l \mathbf{w}^T \mathbf{B}_2^T \mathbf{B}_2 \mathbf{d} N dx = \mathbf{w}^T \underbrace{\int_0^l \mathbf{B}_2^T \mathbf{B}_2 N dx}_{\mathbf{K}_g^e} \mathbf{d}$$

$$(24)$$

The geometric part of the stiffness matrix can also be stated explicitly in form of

$$\mathbf{K}_g^e = \frac{N}{l} \begin{bmatrix} 0 & 0 & 0 & 0 \\ 0 & 1 & 0 & -1 \\ 0 & 0 & 0 & 0 \\ 0 & -1 & 0 & 1 \end{bmatrix} \tag{25}$$

4. General linear eigenvalue problem and solution procedure

The final product of the finite element discretization of geometrical instability problem is a set of algebraic equations that can be written as

$$\mathbf{w}^{eT}\mathbf{f} = \sum_{e=1}^{n} \mathbf{w}^{eT} \underbrace{\left[\mathbf{K}_m^e + \mathbf{K}_g^e\right]}_{\mathbf{K}_t}\mathbf{d} \tag{26}$$

This is indeed a nonlinear problem, since the geometric part of the stiffness is a function of the internal force which further depends upon the displacement at the critical point. However, we can exploit such a special form of the geometric stiffness, which depends linearly upon applied loads to rewrite the geometric stiffness as the product of the load multiplier λ and the reference value $\overline{\mathbf{K}}_g$

$$\mathbf{K}_t = \mathbf{K}_m + \lambda \overline{\mathbf{K}}_g \tag{27}$$

In this manner we indicate that the geometric stiffness matrix involves the state of stress at the critical point, which can be the result of either mechanical or thermal loading. The material part of stiffness matrix depends on material response only, and it can eventually be affected by inelastic behavior of material.

We are interested in dealing with instability phenomena, where the stiffness matrix can become singular. The instability phenomena thus imply that a small perturbation of loading (mechanical, thermal etc.) can lead to a disproportional amplification in computed response. Under a critical force $\mathbf{f}_{cr} = \lambda_{cr}\overline{\mathbf{f}}$ a system is in the critical equilibrium state. At the critical equilibrium state tangent stiffness becomes singular and its determinant will take zero value

$$\det\left(\mathbf{K}_m + \lambda_{cr}\overline{\mathbf{K}}_g\right) = 0 \tag{28}$$

We can further use the solution of such an eigenvalue problem to estimate the critical load. The material stiffness in an elastic material will not change with respect to the case of linearized kinematics since the displacements prior to the critical equilibrium state remain small. The geometric stiffness depends linearly on the load parameter, since the stresses depend linearly on applied load if the displacements are small. The applied mechanical or thermal load is independent of the displacements. At the critical equilibrium state, $\mathbf{K}_t\,\mathbf{\psi}_{cr} = 0$, which implies that for critical mode $\mathbf{\psi}_{cr}$, tangent stiffness matrix $\mathbf{K}_t$ will have a zero eigenvalue. Since the geometric stiffness varies linearly with the load, we can write

$$\left(\mathbf{K}_m + \lambda \overline{\mathbf{K}}_g\right)\mathbf{\psi}_{cr} = 0 \tag{29}$$

where $\overline{\mathbf{K}}_g$ is the geometric stiffness computed for a reference value of the load parameter, $\bar{f}, \bar{\theta}$. The critical value of the load parameter λ_{cr} can be obtained by solving the general eigenvalue problem stated in Eq. (29) above. We note in passing that the same kind of eigenvalue problem appears in dynamics with mass matrix $\mathbf{M}$ replacing $\overline{\mathbf{K}}_g$, and eigenvalue pertinent to the natural frequencies. We will thus borrow the methods already known for efficiency in solving the eigenvalue problem in dynamics, such as the Lanczos method (e.g., see Ibrahimbegovic and Wilson (1990), Ibrahimbegovic *et al.* (1990)).

We note that the present buckling problem can even be solved efficiently simply by using the power method (e.g., Bathe (1996)), given that only the first eigenvalue is usually needed, leading to true critical load. Namely, by using any vector $\mathbf{x}$ (a good starting value should be as close as possible to the first critical mode), we can launch the iterative sequence by

$$\tilde{\mathbf{x}}^{(1)} \to \mathbf{x}^{(1)} = \frac{\tilde{\mathbf{x}}^{(1)}}{\left\|\tilde{\mathbf{x}}^{(1)}\right\|}, \qquad \lambda^{(1)} = \left\|\tilde{\mathbf{x}}^{(1)}\right\| = \sqrt{\left(\tilde{\mathbf{x}}^{(1)}\right)^T \mathbf{M} \tilde{\mathbf{x}}^{(1)}}$$

$$(i) = 1, 2, \ldots \qquad \mathbf{K}_m \tilde{\mathbf{x}}^{(2)} = \lambda^{(1)} \overline{\mathbf{K}}_g \mathbf{x}^{(1)} \quad \to \quad \lambda^{(1)} = \left\|\tilde{\mathbf{x}}^{(2)}\right\|, \qquad \mathbf{x}^{(1)} = \frac{\tilde{\mathbf{x}}^{(2)}}{\left\|\tilde{\mathbf{x}}^{(2)}\right\|} \qquad (30)$$

$$\left|\lambda^{(1)} - \lambda^{(2)}\right| < tol$$

The complete summary of the proposed procedure is as follows. We write the nonlinear equilibrium equation for a special form of external loads

$$\mathbf{f}^{ext} = \overline{\mathbf{f}} \lambda \tag{31}$$

where $\overline{\mathbf{f}}$ is the load reference value and λ is the load multiplier.

We solve for the corresponding reference values of displacement $\mathbf{K}_m \overline{\mathbf{u}} = \overline{\mathbf{f}}$ and then proceed to compute the reference values of internal force $\overline{N}$ in each element, as well as the corresponding reference value of the geometric stiffness $\overline{\mathbf{K}}_g$. Finally, by solving general linear eigenvalue problem in Eq. (29) we compute λ_{cr} along with the critical value of the external loading $\mathbf{f}_{cr} = \lambda_{cr} \overline{\mathbf{f}}$.

When we are dealing with coupled thermomechanical problem, we consider a particular load combination of two load cases – mechanical and thermal loading. First we consider the proportional loads. Solving $\mathbf{K}_m \mathbf{u} = \overline{\mathbf{f}}$, we get displacements caused by this load combination. Once we have the values of displacements, we can calculate corresponding axial forces, and finally form the geometric part of stiffness matrix $\overline{\mathbf{K}}_{g,mech+therm}$. Then we can solve the eigenvalue problem, and get critical value of the load parameter λ_{cr} for the load combination.

$$\left(\mathbf{K}_m + \lambda \overline{\mathbf{K}}_{g,mech+therm}\right) \mathbf{\psi}_{cr} = 0 \tag{32}$$

Next, we are interested in calculating critical value of the load parameter λ_{cr} for one load case only, here for example for thermal load case. Mechanical loads (for example dead loads and some of the live loads) can be considered fixed (their intensity does not change). We apply force f_{mech} on the top of the bar system. Now we can write

$$\mathbf{K}_m \mathbf{u}_{mech} = \mathbf{f}_{mech} \tag{33}$$

Once we obtain displacements caused by mechanical load, we can calculate stresses under mechanical load and its contribution to geometric part of stiffness matrix $\mathbf{K}_{g,mech}$.

We will consider that the thermal load is load case that changes. Same problem as described above in Eq. (33) we are solving for thermal load $\bar{f}_{therm}$. Once we get the geometric part of stiffness matrix $\bar{\mathbf{K}}_{g,therm}$, which depends on stresses caused by thermal load, we can solve next problem and obtain critical value of the load parameter λ_{cr}

$$\left(\underbrace{\mathbf{K}_m + \mathbf{K}_{g,mech}}_{\hat{\mathbf{K}}_m} + \lambda \bar{\mathbf{K}}_{g,therm} \right) \boldsymbol{\psi}_{cr} = 0 \quad \Leftrightarrow \quad \left(\hat{\mathbf{K}}_m + \lambda \bar{\mathbf{K}}_{g,therm} \right) \boldsymbol{\psi}_{cr} = 0 \tag{34}$$

We note that the mechanical load induced geometric stiffness can here act as the pre-stressing increasing the resistance to buckling in a tensile truss-bar or as a factor for reducing the final value of buckling load if truss-bar is compressed.

5. Numerical examples

In this section we consider several numerical examples in order to illustrate the satisfying performance of the proposed method for buckling load computations. All numerical computations were performed by a research version of the computer code FEAP (see Zienkiewicz and Taylor (2005)).

5.1 Validation examples

5.1.1 Simple truss structure under mechanical load
The first example that we will consider for validation of the proposed method for a simple truss-bar structure loaded with mechanical load. The chosen geometric and mechanical characteristics of the structure are given in Table 1 and Fig. 3

$$\bar{N}_1 = \bar{N}_2 = \bar{N} = \frac{1}{2}\frac{l}{h}$$

$$\mathbf{K}_m = \mathbf{K}_m^1 + \mathbf{K}_m^2 = 2\frac{EA}{l}\begin{bmatrix} c^2 & 0 \\ 0 & s^2 \end{bmatrix} \qquad \bar{\mathbf{K}}_g = \bar{\mathbf{K}}_g^1 + \bar{\mathbf{K}}_g^2 = -\frac{1}{l}\frac{1}{s}\begin{bmatrix} s^2 & 0 \\ 0 & c^2 \end{bmatrix}$$

$$\mathbf{K} = \sum_{e=1}^{4}\left(\mathbf{L}^{eT}\mathbf{T}^T\mathbf{K}_m^e\mathbf{T}\mathbf{L}^e - \mathbf{L}^{eT}\mathbf{T}^T\mathbf{K}_g^e\mathbf{T}\mathbf{L}^e \right) \qquad \mathbf{K} = \mathbf{K}_m + \bar{\mathbf{K}}_g = \frac{2EA}{l}\begin{bmatrix} c^2 & 0 \\ 0 & s^2 \end{bmatrix} - \lambda\frac{1}{l}\frac{1}{s}\begin{bmatrix} s^2 & 0 \\ 0 & c^2 \end{bmatrix}$$

Table 1 Mechanical characteristics of the structure

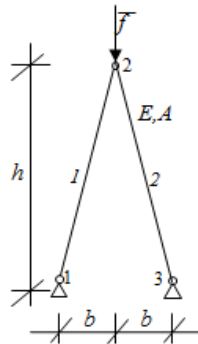| $b[m]$	$h[m]$	$l[m]$	$A[m^2]$	$E[kN/m^2]$	$\bar{f}$ $[kN]$	c	s
0.3	4.0	4.011	10^{-4}	$2 \cdot 10^8$	1.0	b/l	h/l

Fig. 3 Simple truss-bar system example 1

$$\det \mathbf{K} = 0 \Rightarrow \left(\frac{2\mathrm{EA}}{l}c^2 - \lambda \frac{s}{l} \right)\left(\frac{2\mathrm{EA}}{l}s^2 - \lambda \frac{1}{l}\frac{1}{s}c^2 \right) = 0$$

$$\left(\frac{2\mathrm{EA}}{l}c^2 - \lambda \frac{s}{l} \right) = 0 \Rightarrow \lambda_{cr1} = 2\mathrm{EA}\frac{c^2}{s} = \frac{2EA}{l}\frac{b^2}{h} \Rightarrow f_{cr} = \frac{2\mathrm{EA}}{l}\frac{b^2}{h}$$

$$\lambda_{cr1} = \frac{2 \cdot 2 \cdot 10^8 \cdot 10^{-4}}{4,011}\frac{0,3^2}{4} = 224,38 \qquad f_{cr} = \lambda_{cr} \cdot \overline{f} = 224,38 kN$$

$$\left(\frac{2\mathrm{EA}}{l}s^2 - \lambda \frac{1}{s}\frac{c^2}{l} \right) = 0 \Rightarrow \lambda_{cr2} = 2\mathrm{EA}\frac{s^3}{c^2} = \frac{2EA}{l}\frac{h^3}{b^2} = \frac{2 \cdot 2 \cdot 10^8 \cdot 10^{-4}}{4,011}\frac{4^3}{0,3^2} = 709,16 \cdot 10^4$$

Our model in FEAP gave us the same results:
$$\lambda_{cr1} = 2.24369845D + 00$$
$$\lambda_{cr2} = 7.09119509D + 04$$

We have thus got validation for mechanical part.
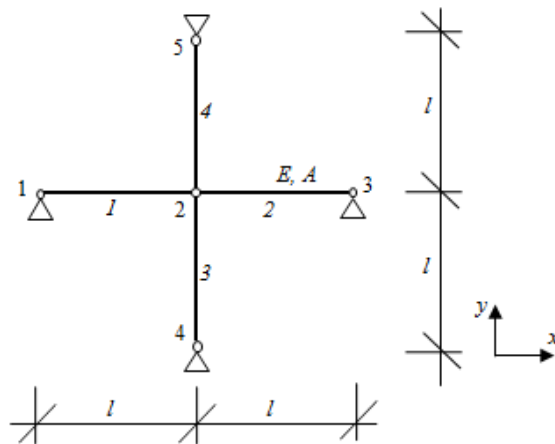
Fig. 4 Truss bar system example 2

5.1.2 Simple truss under thermal load

Let us consider an example of a truss bar system, given in Fig. 4. All bars are the same length l and cross section A, subjected to a constant temperature $\bar{\theta}$. We assume that material properties are independent on temperature. Due to temperature load, axial force $N = EA\alpha\theta$ occurs in bars.

Vector of unknown displacements: $u = \left\{ \begin{matrix} u_2 \\ v_2 \end{matrix} \right\}$, u is displacement in direction x, and v in direction y.

Tangent stiffness matrix of a bar element can be obtained by: $\left[\mathbf{K}^e \right] = \left[\mathbf{K}_m^e \right] + \left[\overline{\mathbf{K}}_g^e \right]$

Here, $\mathbf{K}_m$ is the material, or elastic part of stiffness matrix, and $\mathbf{K}_g$ is the geometric part of the stiffness matrix

$$\mathbf{K}_m^e = \frac{EA}{l} \begin{bmatrix} 1 & 0 & -1 & 0 \\ 0 & 0 & 0 & 0 \\ -1 & 0 & 1 & 0 \\ 0 & 0 & 0 & 0 \end{bmatrix} \qquad \overline{\mathbf{K}}_g^e = \frac{N}{l} \begin{bmatrix} 0 & 0 & 0 & 0 \\ 0 & 1 & 0 & -1 \\ 0 & 0 & 0 & 0 \\ 0 & -1 & 0 & 1 \end{bmatrix}$$

$$\mathbf{K} = \sum_{e=1}^{4} \left(\mathbf{L}^{eT} \mathbf{K}_m^e \mathbf{L}^e - \mathbf{L}^{eT} \overline{\mathbf{K}}_g^e \mathbf{L}^e \right)$$

$$\mathbf{K} = \frac{2EA}{l} \begin{bmatrix} 1 & 0 \\ 0 & 1 \end{bmatrix} - \frac{2N_t}{l} \begin{bmatrix} 1 & 0 \\ 0 & 1 \end{bmatrix} \qquad \mathbf{K} = \underbrace{\begin{bmatrix} \dfrac{2EA}{l} - \lambda \dfrac{2N_t}{l} & 0 \\ 0 & \dfrac{2EA}{l} - \lambda \dfrac{2N_t}{l} \end{bmatrix}}_{\det[\cdot]=0}$$

$$\det \left[\mathbf{K}_m - \lambda \overline{\mathbf{K}}_g \right] = 0 \qquad \frac{2EA}{l} - \lambda \frac{2N_t}{l} = 0 \qquad \lambda = \frac{EA}{N_t}$$

$$\lambda_{cr1,2} = \frac{1}{\alpha\theta} = \frac{1}{10^{-5} \cdot 40} = 2500$$

Results obtained by the model in FEAP: $\lambda_{cr1} = \lambda_{cr2} = 2.50000000\,\mathrm{D} + 03$

In this manner, we have also got validation for thermal part.

5.2 Tower instability under mechanical and thermal load

We further will deal with coupled thermomechanical problems. Any real structure (e.g., a tower in Fig. 5) is designed to withstand mechanical loads, first including the dead load. The thermal load comes from different kinds of accidents that can cause fire in structures. Here we would like to check the risk of instability phenomena under combined thermomechanical loads of this kind.

Given that if we consider a multistory structure, of special interest is the case where the fire is located only on one floor.

In this example we will consider the instability of the tower given in Fig. 5, under coupled thermomechanical loads. The mechanical load is always the same with a single concentrated force

applied on top. However, different thermal loads are considered: i) with increase of temperature in outside bars only throughout the tower height, ii) the temperature increase in the second storey of the tower.

5.2.1 Tower instability under mechanical loads only
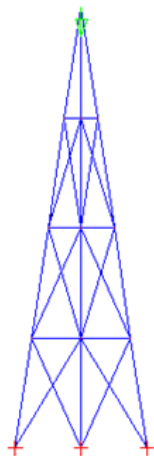In this case, the system is loaded only by a mechanical force applied at the top of the structure

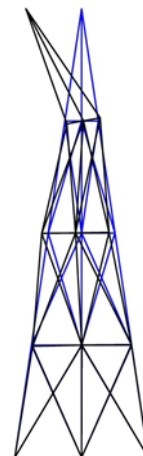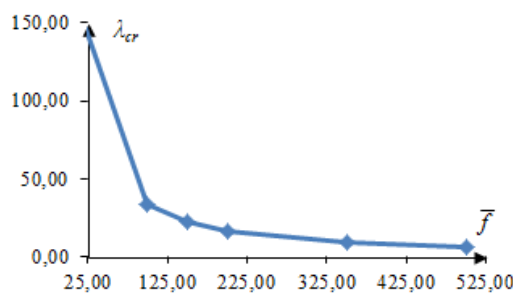Fig. 5 Initial configuration of the tower
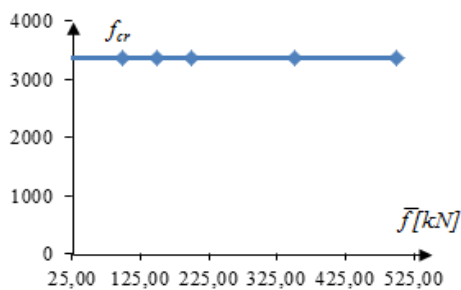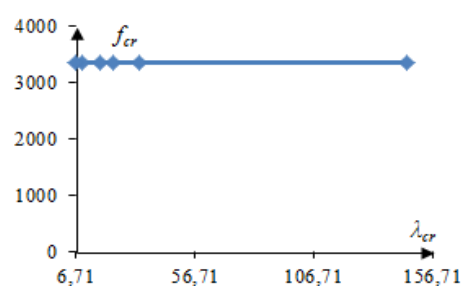

Fig. 6 Buckling mode

Fig. 7 Critical load multiplier – mechanical load curve

(a) Critical load – mechanical load curve

(b) Critical load – critical load multiplier curve

Fig. 8 Critical load change

(see Fig. 5). We performed several computations of the critical load for different force intensity, in order to get the corresponding value of critical load multiplier. Each of those computations resulted with the same buckling mode shown in Fig. 6. The change of critical load multiplier as a function of mechanical load is presented in Fig. 7. In Fig. 8(a) we can see that critical load does not depend on reference load intensity.

5.2.2 Tower instability under thermal load – heating of outside bars

We further study instability problem when outside bars of the tower are heated throughout tower height. The bars of the system, undergoing heating are marked in Fig. 9(a) in red. We tested behavior of the critical load multiplier and the critical thermal load for different values of reference temperature. The results are given in figures that follow.

The buckling mode of the system, in the case when outside bars of the system are heated, is shown in Fig. 9(b). Fig. 10 shows the change of the critical load multiplier with respect to temperature change. In Fig. 11(a) we can see that the critical load is independent of chosen reference temperature change.

(a) Initial configuration (b) Buckling mode
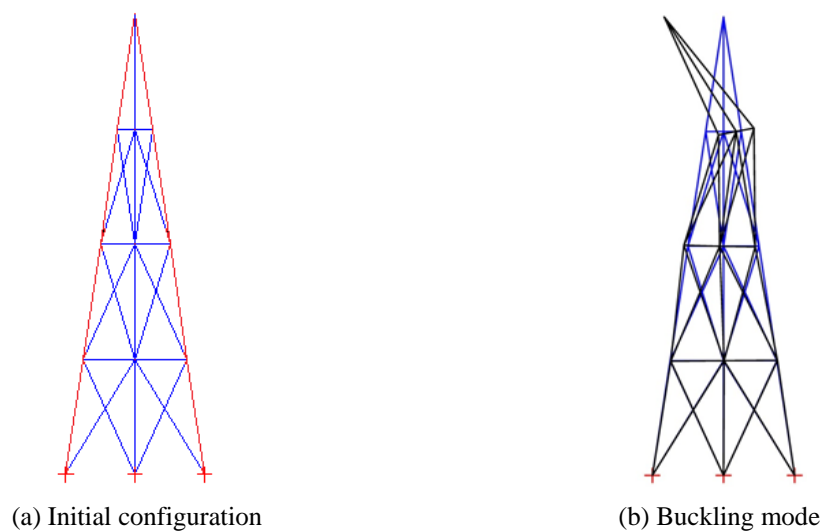
Fig. 9 Tower under thermal load

Fig. 10 Critical load multiplier – thermal load curve
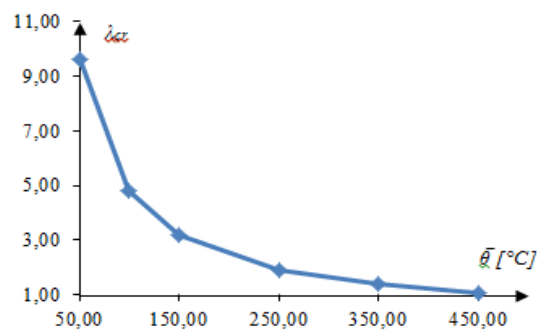
(a) Critical load – mechanical load curve   (b) Critical load – critical load multiplier curve

Fig. 11 Critical load change
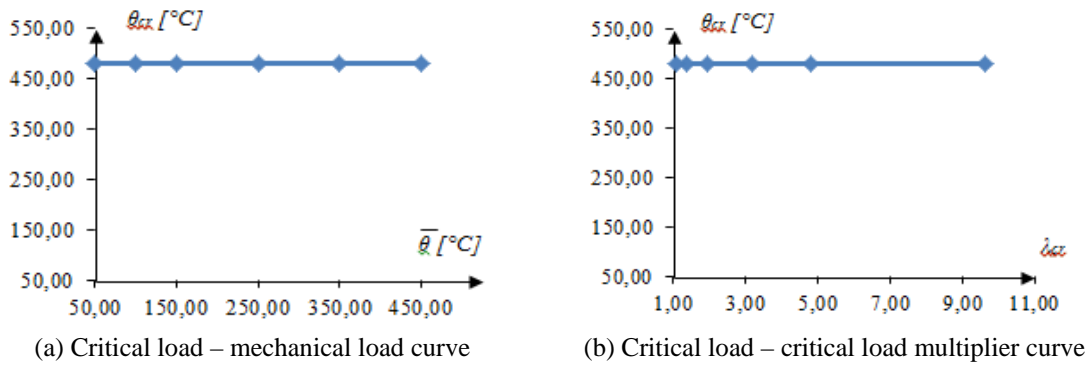
(a) Initial configuration   (b) Buckling mode
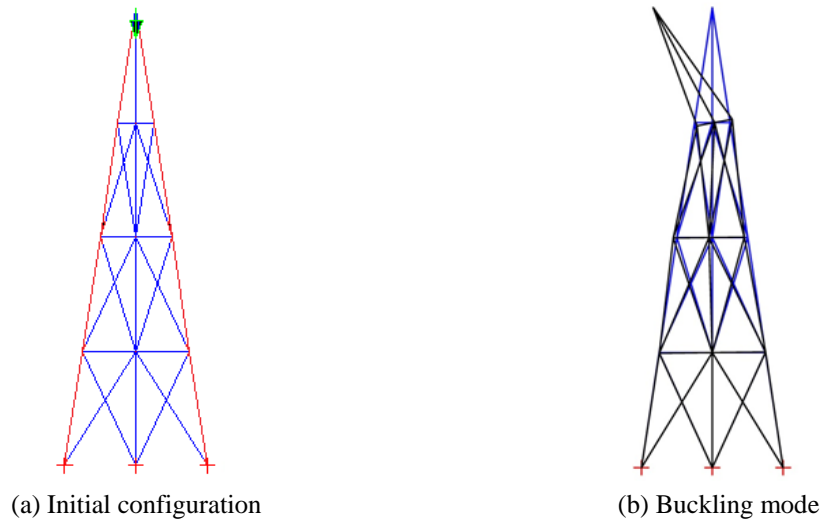
Fig. 12 Tower under coupled mechanical and thermal loads

Fig. 13 Critical load multiplier – thermal load curve

<div align="center">
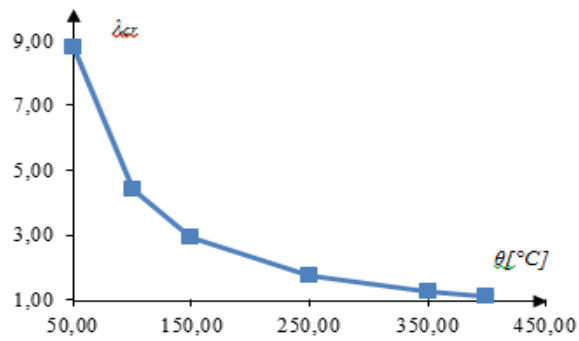
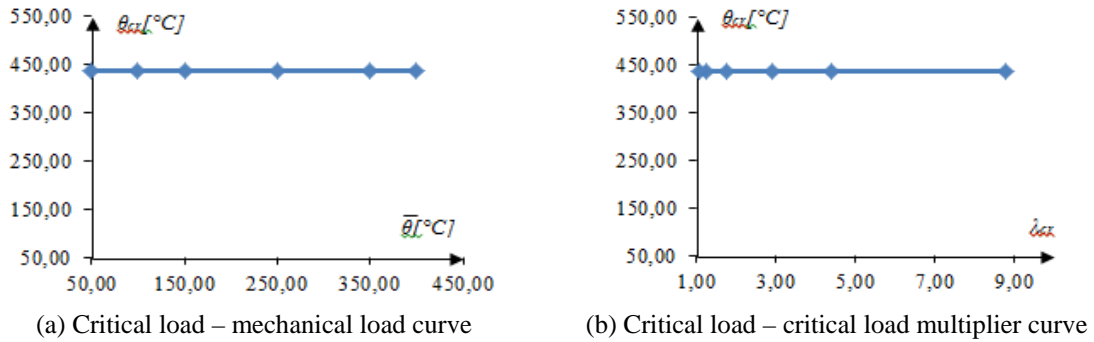(a) Critical load – mechanical load curve　　　　(b) Critical load – critical load multiplier curve

Fig. 14 Critical load change

</div>

5.2.3 Tower instability under coupled mechanical and thermal loads – heating of outside bars

The following analyses were carried out for constant value of mechanical load, and for different values of the temperature. We considered the same truss-bar structure, loaded with constant mechanical load on the top of the system $\bar{f}_{mech}$, and then the red bars in Fig. 12(a) were heated. For different temperature values, the critical load parameter λ_{cr} was calculated. In Fig. 13 it can be seen that the critical load does not change with temperature.

In Fig. 14(a) we have shown change of the critical load parameter with respect to temperature, for constant mechanical load value. Buckling mode for this case is given in Fig. 12(b).

We can note that the critical mode assembles the one computed for mechanical load in Fig. 6 and Fig. 9(b) for thermal load. Thus, there is an increased risk of structure sensitivity to buckling for combined of these two modes. It is interesting to note that similarity of these two buckling modes allow to obtain the same critical load values of f_{cr} and θ_{cr} if the of reference load role is between switched mechanical and thermal loads.
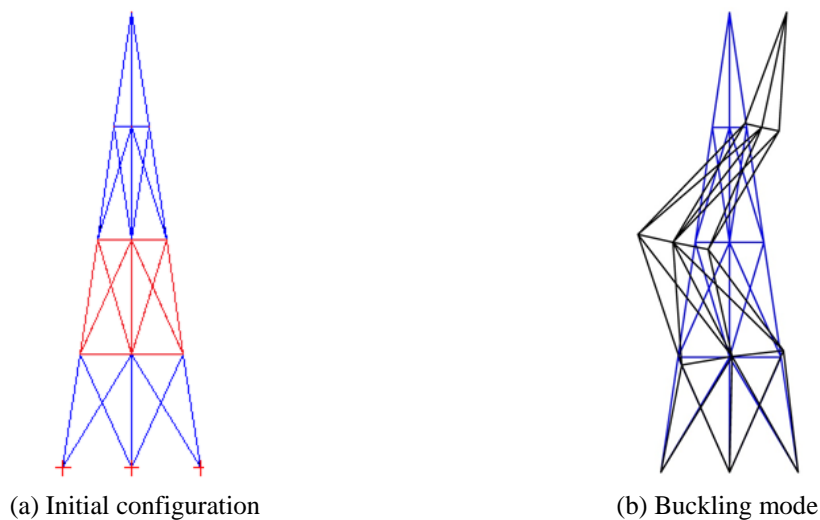

<div align="center">

(a) Initial configuration　　　　　　　　　　(b) Buckling mode

Fig. 15 Tower under thermal loads

</div>

Fig. 16 Critical load multiplier – thermal load curve

(a) Critical load – mechanical load curve   (b) Critical load – critical load multiplier curve
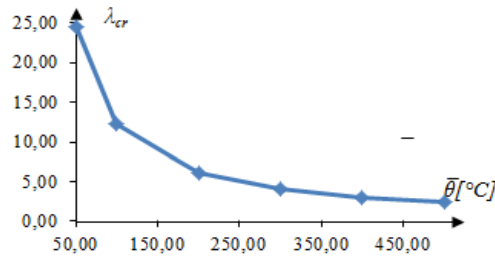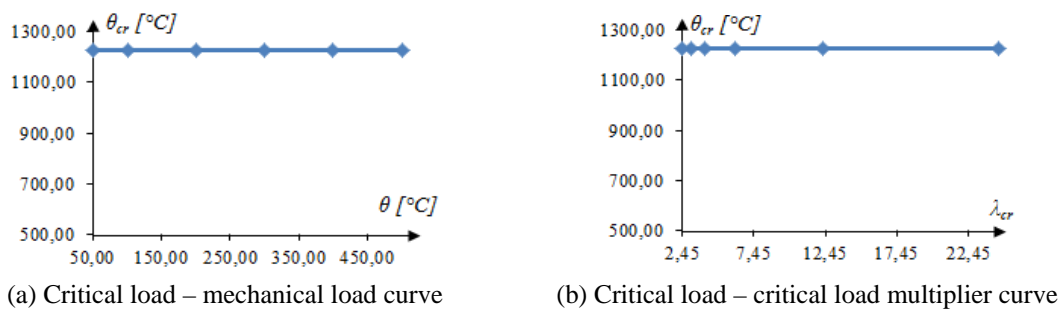
Fig. 17 Critical load change

5.2.4 Tower instability under thermal load – heating one floor

Next, we change the thermal load with heating one floor of the structure. The bars of the structure, marked in Fig. 15(a) with red color undergo heating in this case correspond to the second floor. We tested the change of the critical load multiplier and the critical thermal load with temperature change.

In the case when we were heating only one storey bars, obtained buckling mode of the system is given in Fig. 15(b). The change of the critical load multiplier with respect to temperature change is shown in Fig. 16. The critical load is independent of temperature change, which can be seen in Fig. 17(a).

5.2.5 Tower instability under coupled mechanical and thermal load - heating one floor

In this example we study the coupled thermomechanical problem where fire in structure is localized only in one part of the structure. Here, the temperature is rising, while mechanical loads stay unchanged. We will consider the same truss-bar structure loaded with constant mechanical load on the top of the structure. The bars which are submitted to heating are shown in Fig. 18(a) in red color.

In Fig. 18(b) we can see buckling mode for this analysis case, and it shows that influence of temperature is dominant in response. In fact, by comparison of instability mode for mechanical case shown in Fig. 6 and buckling mode for local temperature change shown in Fig. 15(b), we can see that the combined loads instability is mostly characterized by the latter. We thus conclude that the local temperature change with only one storey exposed to fire will not have the same resonance effect as in the previous example. Furthermore, if the order is reversed, with one storey temperature change kept fixed while increasing mechanical loads until critical value we do not obtain the same critical loads values.
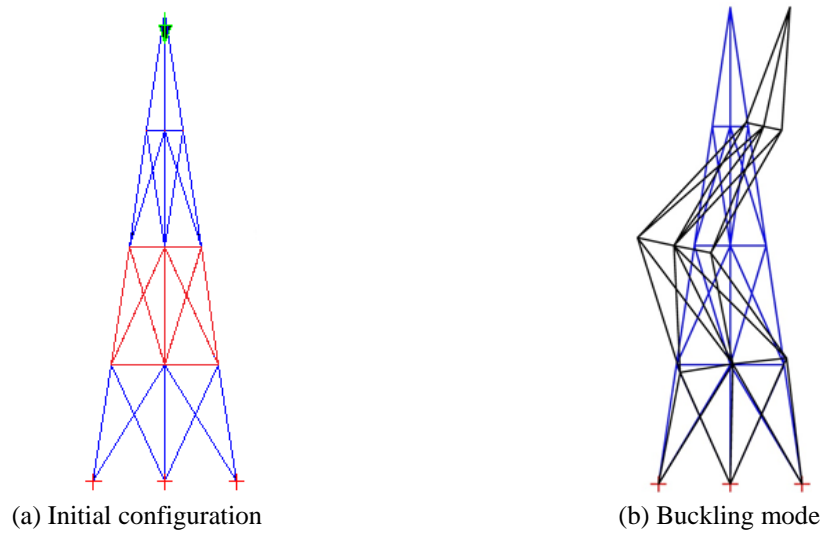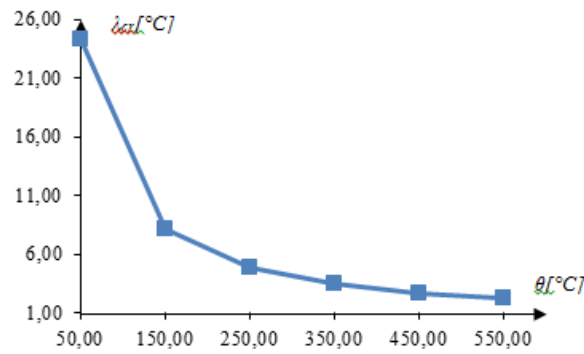
(a) Initial configuration   (b) Buckling mode

Fig. 18 Tower under coupled mechanical and thermal loads
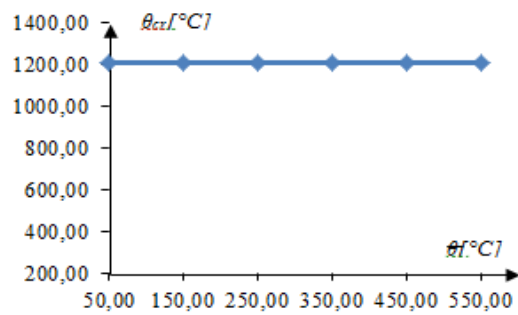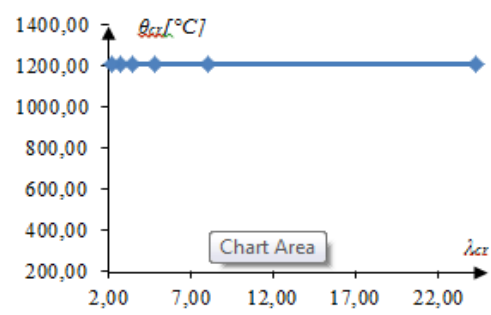

Fig. 19 Critical load multiplier – thermal load curve

(a) Critical load – mechanical load curve   (b) Critical load – critical load multiplier curve

Fig. 20 Critical load change

5.3 Comparison against finite strain elasticity model

Next, we will compare values of critical forces we obtained in previous chapters against results of finite strain elasticity model (see Appendix). First, we will compare simple truss structure from validation example (Fig. 3). An analysis was performed using finite strain model, and we obtained force-displacement curve presented in Fig. 21. Curve shows values of vertical force and vertical

Table 2 Mechanical characteristics of the structure

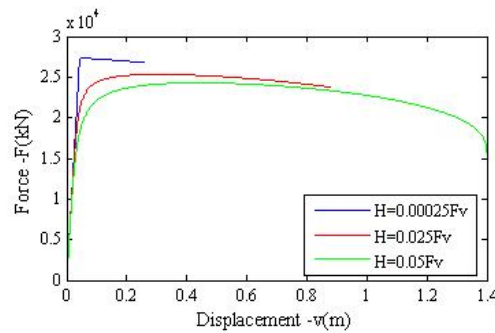| b[m]	h[m]	l[m]	A[m^2]	E[kN/m^2]	λ_{cr}
0.3	4.0	4.011	10^{-4}	$2 \cdot 10^8$	224.37
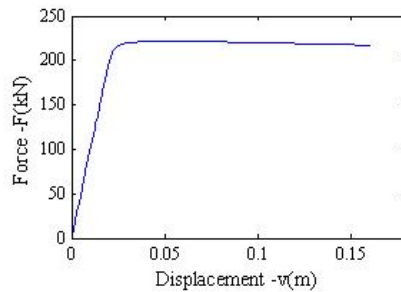
Fig. 21 Force-displacement curve

Fig. 22 Force-displacement curve (different horizontal forces)
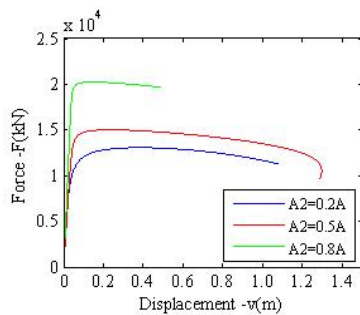

Fig. 23 Force-displacement curve (changing cross section of the tower's left side bars)
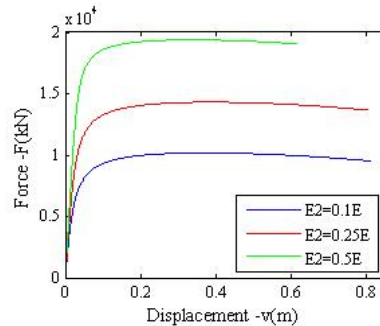
Fig. 24 Force-displacement curve (changing Young's modulus of the tower's left side bars)
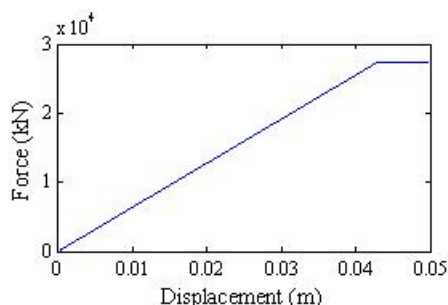
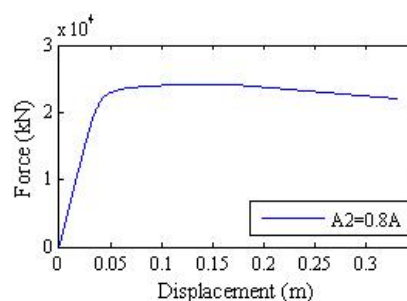Fig. 25 Force-displacement curve (perturbation caused by horizontal force)

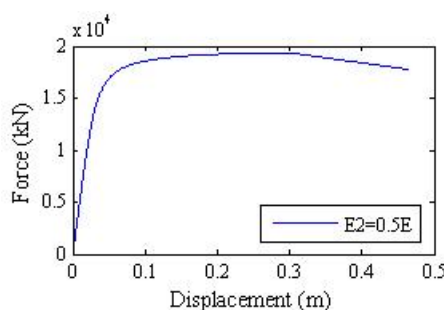Fig. 26 Force-displacement curve (perturbation caused by cross section change)

Fig. 27 Force-displacement curve (perturbation caused by Young's modulus change)

displacement of node 2 (see Fig. 3). While performing nonlinear analysis, we had to apply small horizontal perturbation in order to disturb the symmetry of the truss structure.

Critical force was computed using the arc-length method (e.g., Ibrahimbegovic (2009)), and its value is f_{cr} = 221,54 kN. In 5.2.1 is given critical force value obtained by linear computation, f_{cr} = 224,37 kN. These two values are approximately the same, which gives us validation of obtained results. In the case of incremental analysis force f_{cr} = 218,63 kN was obtained.

In order to get full validation of our results and models, we performed couple of tests on this simple truss structure. We tested behavior of the truss in case when symmetry is disturbed in manner that one bar has smaller cross section (A_2 = 0,95A), and also the case when bars have equal cross sections, but different Young's modulus (E_2 = 0,95E). Using the arc-length method critical force f_{cr} = 216,11 kN was computed for both cases, and using incremental analysis force f_{cr} = 216,00 kN was obtained.

The similar comparison as shown above, we performed for tower given in Fig. 5. First, we performed nonlinear analysis only with mechanical load applied (see Fig. 5). In order to obtain the loss of stability we performed several analyses with different kinds of perturbation. First type of perturbation we used is horizontal force applied on the top of the tower. We made couple of computations varying horizontal force intensity. In the Fig. 22 are presented force-displacement curves: force on the top of the tower, and displacement of the same node.

Then we changed a cross section of the bars on the left side of the tower, and in that manner we disturbed symmetry. Force-displacement curves are given in Fig. 23. The final way in which we disrupted symmetry of the tower was reducing of the Yang's modulus of the bars on the left side of the tower, computed results are shown in Fig. 24.

Above results are obtained using the arc-length method. We also made similar computations using incremental method. Horizontal force, the change of cross section, and the change of Young's modulus were used as perturbations. Obtained results are shown in Figs. 25- 27.

Here, we will also show how results change with slenderness of the truss.

In Table 3 are given values of the critical force obtained by linear and nonlinear analysis, for different *h/b* (height/base) ratio. We can notice that larger the ratio *h/b*, the smaller difference between the critical force values obtained by two models (linear and nonlinear).

Comparing results obtained using finite strain elasticity model with results computed in 5.2, one can see significant differences. We can conclude that it would be necessary to refine the mesh, but this is not possible using truss elements.

Table 3 Critical force values

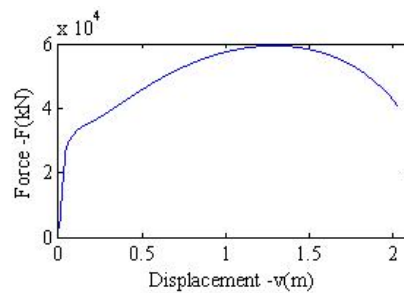| Model	h/b	3.33	6.67	8.33	10
Linear	f_{cr} *[kN]*	3356.6	2970.0	1938.6	1358.2
Nonlinear		27414.0	6984.0	4480.0	3115.0

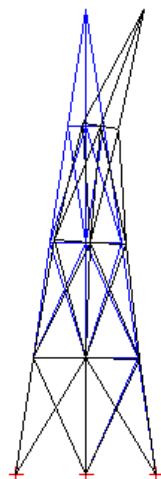Fig. 28 Force-displacement curve
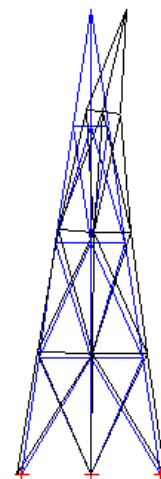

Fig. 29 Buckling mode

Fig. 30 Deformed shape in time when instability occurs

5.4 Tower instability using frame elements

In order to prove that accuracy of the results given in 5.3 is mesh-dependent, we will consider the same tower loaded with force on the top, but model composed by using the frame elements. First, we will use simple mesh, the same we used when tower was modeled with truss elements.

Force-displacement curve is given in Fig. 28. In Fig. 29 is given buckling mode of tower. Fig. 30 shows the deformed shape of the tower obtained using finite strain elasticity model, in time when buckling occurs.

Critical values of force and displacement are given in Table 4.

We can see that critical values obtained using linear and finite strain model are significantly different, just like in case when truss elements were used.

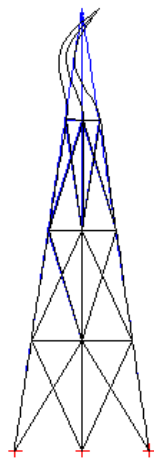| Table 4 Critical force and displacement values			Table 5 Critical force and displacement values		
Model	f_{cr} *[kN]*	v_{cr} *[m]*	*Model*	f_{cr} *[kN]*	v_{cr} *[m]*
Linear	30490,7	-4,635E-02	*Linear*	16439,0	-2,517E-02
Nonlinear	59375,0	-1,2920	*Nonlinear*	16175,0	-2,558E-02

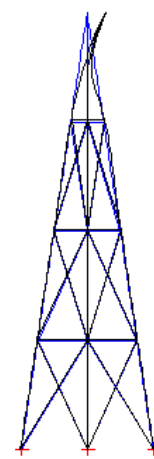Fig. 31 Buckling mode (refined mesh)

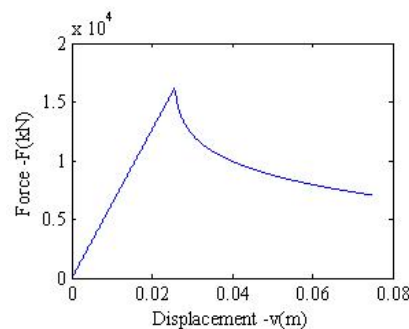Fig. 32 Deformed shape in time when instability occurs (refined mesh)

Fig. 33 Force-displacement curve (refined mesh)

The same analysis is performed for the tower with refined mesh. All frames from previous case are divided in 19 elements. New values of critical force and critical displacement are obtained and the results are given in Table 5.

We can see that obtained results, after the mesh is refined, are nearly the same for linear and nonlinear analysis. Therefore, we can conclude that the same problem exists using truss elements, which gives us explanation for differences in critical force values in 5.3. Since using truss elements, mesh cannot be further refined, we are not able to obtain matching results.

5. Conclusions

In this paper, a model for instability failure under thermomechanical loads is introduced. The model is capable of modeling the behavior of structure subjected to mechanical and thermal loading. The main novelty of the proposed model is its capability to account for geometric nonlinearities, based upon the von-Karman strain measure, under mechanical or combined thermomechanical loads. The corresponding generalized eigenvalue problem for direct estimate of the critical load leading to instability and failure is introduced. We considered small pre-buckling displacements, which leads to linear kinematics and nonlinear equilibrium equations. We introduced the finite element method dealing buckling problems. It is shown that such a critical value of load parameter can be obtained by solving the general eigenvalue problem.

The numerical examples have shown that response of the structure depends on the part of the structure where the fire is located. The first buckling mode of the tower for mechanical loads only can sometimes be in a "resonance" with the buckling mode for fire loading. The case in point is the uniform heating of overall structure. On the other hand, for the case of localized fire the buckling load correspond to the higher order buckling mode for mechanical loads only. It is thus very important to define the most precise load combination and the corresponding loading program when computing the estimates of buckling mode for coupled thermomechanical loading.

Acknowledgements

References

Bathe, K.J. (1996), *Finite Element procedures*, Prentice-Hall, Englewood Cliffs, NJ, USA.
Dujc, J., Brank, B. and Ibrahimbegovic, A. (2010), "Multi-scale computational model for failure analysis of metal frames that includes softening and local buckling", *Comp. Meth. Appl. Mech. Eng.*, **199**(21-22), 1371-1385.
Ericsken, J. (1998), *Introduction to the Thermodynamics of Solids*, Springer, Berlin, Germany.
Ibrahimbegovic, A. (2009), *Nonlinear Solid Mechanics: Theoretical Formulations and Finite Element Solution Methods*, Springer, Berlin, Germany.
Ibrahimbegovic, A. and Al Mikdad, M. (2000), "Quadratically convergent direct calculation of critical points for 3d structures undergoing finite rotations", *Comp. Meth. Appl. Mech. Eng.*, **189**(1), 107-120.
Ibrahimbegovic, A. and Chorfi, L. (2000), "Viscoplasticity model in finite deformations with combined isotropic and kinematic hardening", *Comput. Struct.*, **77**(5), 509-525.

Ibrahimbegovic, A. and Chorfi, L. (2002), "Covariant principal axis formulation of associated coupled thermoplasticity at finite strains and its numerical implementation", *Int. J. Solids. Struct.*, **39**(2), 499-528.

Ibrahimbegovic, A. and Wilson, E.L. (1990), "Automated truncation of Ritz vector basis in modal transformation", *J. Eng. Mech. – ASCE*, **116**(11), 2506-2520.

Ibrahimbegovic, A., Chen, H.C., Wilson, E.L. and Taylor, R.L. (1990), "Ritz method for dynamic analysis of linear systems with non-proportional damping", *Earthq. Eng. Struct. D.*, **19**(6), 877-889.

Ibrahimbegovic, A., Chorfi, L. and Gharzeddine, F. (2001), "Thermomechanical coupling at finite elastic strain: Covariant formulation and numerical implementation", *Numer. Meth.*, **17**(4), 275-289.

Ibrahimbegovic, A., Colliat, J.B. and Davenne, L. (2005), "Thermomechanical coupling in folded plates and non-smooth shells", *Comp. Meth. Appl. Mech. Eng.*, **194**(21-24), 2686-2707.

Ibrahimbegovic, A., Shakourzadeh, H., Batoz, J.L., Al Mikdad, M. and Guo, Y.Q. (1996), "On the role of geometrically exact and second order theories in buckling and post-buckling analysis of three-dimensional beam structures", *Comput. Struct.*, **61**(6), 1101-1114.

Ngo, V.M., Ibrahimbegovic, A. and Brancherie, D. (2013), "Model for localized failure with thermo-plastic coupling: Theoretical formulation and ED-FEM implementation", *Comput. Struct.*, **127**, 2-18.

Timoshenko, S.P. and Gere, J.M. (1962), *Theory of Elastic Stability*, (2nd Edition), McGraw-Hill Co., New York, USA.

Yang, Y.B., Lin, T.J., Leu, L.J. and Huang, C.W. (2008), "Inelastic postbuckling response of steel trusses under thermal loadings", *J. Constr. Steel. Res.*, **64**(12), 1394-1407.

Zienkiewicz, O.C. and Taylor, R.L. (2005), *The Finite Element Method*, Vols. I, II, III, Elsevier, Oxford, UK.

CC

Appendix

Thermomechanical coupling for 1D finite elasticity

In order to illustrate theoretical description of thermomechanical coupling in large strain elasticity, we start with the simplest 1D problem, considering elastic truss bar. The deformed shape of such a bar, stretched along *x*-axis, can be defined by the position vector

$$\varphi(x,t) = x + d(x,t)$$

where *x* is an independent variable of space, and *t* is the pseudo-time parameter which describes chosen loading program, $d(x,t)$ is the displacement along the bar axis. The stretch $\lambda(x,t)$ defined at each point *x*

$$\lambda(x,t) = \frac{\partial \varphi(x,t)}{\partial x}$$

Equilibrium equation in the deformed configuration can be written

$$0 = \frac{\partial P(x,t)}{\partial x} + b(x,t)$$

where *P* is the first Piola-Kirchhoff stress and *b* distributed loading per unit length of initial configuration.

If we write internal energy potential in a form

$$\varepsilon = ln\lambda \qquad e(\varepsilon, s)$$

We can establish the local form of the first principle of thermodynamics. The first principle of thermodynamics states that any change of the internal energy is proportional to the combined effects of the stress power and the heat supply

$$\underbrace{\frac{\partial}{\partial t} e(\lambda, s)}_{\frac{\partial e}{\partial \varepsilon}\frac{\partial \varepsilon}{\partial t} + \frac{\partial e}{\partial s}\frac{\partial s}{\partial t}} = \underbrace{P \frac{\partial \lambda}{\partial t}}_{\tau \frac{\partial \varepsilon}{\partial t}} + r - \frac{\partial q_0}{\partial x}$$

The last result can be rewritten

$$\left(\frac{\partial e}{\partial \varepsilon} - \tau \right) \frac{\partial \varepsilon}{\partial t} + \frac{\partial e}{\partial s}\frac{\partial s}{\partial t} = r - \frac{\partial q_0}{\partial x}$$

One can avoid working with the entropy as independent variable by making use of the Legendre transformation which gives rise to the Helmholtz free energy and switches the roles between entropy and temperature.

$$\psi(\varepsilon, \theta) = e(\varepsilon, s) - s\theta$$

The first principle of thermodynamics can then be restated as

$$\left(\frac{\partial \psi}{\partial \varepsilon} - \tau\right)\frac{\partial \varepsilon}{\partial t} + \left(\frac{\partial \psi}{\partial \theta} + s\right)\frac{\partial \theta}{\partial t} + \theta\frac{\partial s}{\partial t} = r - \frac{\partial q_0}{\partial x}$$

We can further introduce the free energy potential

$$\psi(\varepsilon, \theta) = \underbrace{\frac{1}{2}\varepsilon E \varepsilon}_{\bar{\psi}(\varepsilon)} + \underbrace{c\left[(\theta - \theta_0) - \theta ln\frac{\theta}{\theta_0}\right]}_{T(\theta)} + \underbrace{\alpha E(\theta - \theta_0)\varepsilon}_{M(\varepsilon, \theta)}$$

We can obtain the corresponding constitutive equations for the Kirchhoff stress including the thermal stress component, as well as the entropy for the elastic processes

$$\tau := \frac{\partial \psi}{\partial \varepsilon} = \underbrace{E\varepsilon}_{\frac{\partial \bar{\psi}}{\partial \varepsilon}} \underbrace{-\alpha E(\theta - \theta_0)}_{\frac{\partial M}{\partial \varepsilon}}$$

$$s := \frac{\partial \psi}{\partial \theta} = \underbrace{-cln(\theta/\theta_0)}_{\frac{\partial T}{\partial \theta}} \underbrace{-\alpha E\varepsilon}_{\frac{\partial M}{\partial \theta}}$$

The weak form of the mechanical part of the coupled problem in thermoplasticity can be written

$$0 = G_M(\varphi, \theta, w) := \int_l \left(w\rho\ddot{\varphi} + \frac{1}{\lambda}\frac{dw}{dx}\tau - wb\right)dx - w(l)\bar{t}$$

$$0 = G_T(\varphi, \theta, \vartheta) := \int_l \vartheta\left(\theta\dot{s} - r + \frac{\partial q_0}{\partial x}\right)dx$$

The linearized version of the mechanical part leads to

$$lin[G_M] = G_M + \underbrace{\frac{d}{d\alpha}[\varphi_\alpha, \theta, w]}_{A} \quad \Rightarrow \quad A = \int_l \left(\frac{1}{\lambda}\frac{dw}{dx}\underbrace{\frac{\partial \tau}{\partial \varepsilon}}_{E}\frac{1}{\lambda}\frac{du}{dx} - \frac{1}{\lambda^2}\tau\frac{dw}{dx}\frac{du}{dx}\right)dx$$

The instability criterion in terms of the singularity of the tangent stiffness matrix remains the same. However, the tangent stiffness remains highly nonlinear function of applied load multiplier, and we can no longer solve this problem with the same efficiency as for the case of the buckling. Another effect that is nonlinear is the temperature with nonstationary flow.